

## Effective reduction of building heat loss without insulation materials via the photothermal effect of a chlorophyll thin film coated “Green Window”

Yuan Zhao, Andrew W. Dunn, and Donglu Shi, The Materials Science and Engineering Program, Department of Mechanical and Materials Engineering, College of Engineering and Applied Science, University of Cincinnati, Cincinnati, OH 45221, USA

Address all correspondence to Donglu Shi at [donglu.shi@uc.edu](mailto:donglu.shi@uc.edu)

(Received 28 January 2019; accepted 9 April 2019)

### Abstract

One of the critical components of energy savings in buildings is thermal insulation, especially for windows in cold climates. The conventional approach mainly relies on a double-pane design. In this study, a new concept of “Green Window” has been designed for single-pane applications that lower the U-factor. The “Green Window” is structurally and simply composed of a thin film window coating of chlorophyll that exhibits pronounced photothermal effect, while remaining highly transparent. We demonstrate a new concept in “thermal insulation” via optical means instead of solely through thermal insulators or spectral selectivity. This concept lifts the dependence on insulating materials making single-pane window highly possible.

### Introduction

Energy efficiency has to be enhanced by reducing the amount of energy required to provide products and services. In energy saving, one critical issue deals with a large amount of heat loss from public buildings, especially in cold regions. According to a report by the US Department of Energy, building heating, ventilation, and air conditioning (HVAC) accounted for 14.0% of primary energy consumption in the USA. Heat loss through windows in cold weather consumes about 3.9 quads, which is estimated to encompass 28.7% of total HVAC energy consumption.<sup>[1]</sup> To quantify overall heat flow through windows, the National Fenestration Rating Council (NFRC) has introduced an energy-performance characteristic of windows: the rate of heat loss, or U-factor. The lower U-factor implies better thermal resistance, meaning the heat flow from a warmer room to the colder outside can be better resisted. The current approach in improving window U-factor has been through either spectral selectivity or structural architecture. The former has been mainly achieved, to a limited extent, via low-emissivity (low-E) coating, while the latter by multiple layers of insulation (double-pane or triple-pane).<sup>[2,3]</sup> Most of the thermally insulated windows in cold climate regions are double-paned, sandwiching transparent insulating materials, such as gases, liquid crystals, vacuum glazing, etc., which creates additional and unnecessary volume and weight, as well as higher cost of the materials.<sup>[4,5]</sup> Therefore, ARPA-E raised the SHIELD program (Single-Pane Highly Insulating Efficient Lucid Designs), aiming at single-pane windows to replace multi-pane windows, includes double-panes and triple-panes.<sup>[1]</sup>

U-factor is proportional to the temperature difference,  $\Delta T$ , between the center of the room and the window interior surface. Therefore, a simple strategy is to slightly raise the window interior surface temperature through the photothermal effect against the colder external environment by collecting solar light that is largely unutilized. Some noble metals, such as gold nanorods, are well known for their pronounced photothermal effects.<sup>[6]</sup> However, these materials often suffer from high absorption in the visible region. A functional coating would be quite plausible if it significantly heats under solar illumination, to lower the U-factor, without involving any insulating materials but retains high visible transparency.

Solar light is an electromagnetic wave of a wide frequency range (from UV to infrared). The photothermal effect is known to be frequency-dependent, leading to varied energy conversion efficiency.<sup>[7]</sup> Furthermore, the intensity of solar light is not uniform with the non-visible light [ultraviolet (UV), near-infrared (NIR), and infrared] counting for more than half of the total solar energy at sea level.<sup>[8]</sup> Ideally, an energy-efficient window should absorb most of the “free” non-visible light and convert it to thermal energy while allowing high visible transmittance (VT). A typical VT ranges between 30% and 80% for most of the double-pane windows.<sup>[9,10]</sup> An energy-efficient window with a low U-factor is optically characterized by a saddle-shaped absorption spectrum, with high absorptions at both edges (UV and NIR) of the visible range for strong photothermal effects. With this concept, unique photothermal coating materials can be developed that collect most of the solar light for self-heating with minimum VT losses. Zhao et al. reported photothermal coatings with  $\text{Fe}_3\text{O}_4$  nanoparticles on glass

substrates that exhibited strong self-heating, irradiated by both NIR laser and solar light, and significantly lowered the U-factor.<sup>[7]</sup> However, VT was negatively impacted. It is therefore important to search for a highly transparent coating with a strong photothermal effect.

In this study, we report a “Green Window” concept based on the natural material chlorophyll (Chl) developed by using a straightforward spin-coating technique on glass that exhibits excellent photothermal effect and high visible transparency. The photothermal effects were investigated on these Chl films by solar light and NIR laser irradiation. Optical properties of the Chl films were characterized including heating curves, optical absorptions, and VT.

The concept of the photothermal “Green Window” is schematically illustrated in Fig. 1 and is a new concept in preventing heat loss, particularly useful for developing single-pane windows. Under solar light, sufficient self-heating can effectively increase the inner window surface temperature, leading to reduced  $\Delta T$  and therefore effectively lowering the U-factor without additional insulating layers between the double-panes. The key factor in energy saving relates to the intensity of the photothermal effect from the thin film coatings on the window glass. Although several materials have been found to exhibit strong photothermal effects, such as gold,  $\text{Fe}_3\text{O}_4$ , and graphene, their optical absorption characteristics are not ideal for window applications.<sup>[11–14]</sup> Figure 2 shows the absorption spectra of various materials indicated. As can be seen in this figure, while gold exhibits strong absorption below 300 nm, there is another peak at 520 nm, contributing to considerable visible light absorption. Much stronger absorption is observed in the

UV range for graphene and  $\text{Fe}_3\text{O}_4$  nanoparticles, but they gradually decay to the minimum in the visible range up to NIR. However, Chl shows the saddle-like spectrum with two peaks, respectively, at 400 nm (blue-violet) and 700 nm (NIR), which is consistent with its green color from which the name “Green Window” is derived.<sup>[15]</sup> It is this typical spectrum with the saddle-like shape that qualifies Chl for making green windows.

## Results and discussion

### Optical absorption characteristics and photothermal effect of chlorophyll

Chl was extracted from local fresh spinach. A detailed extraction process is presented in the Supporting materials. The green solid curve in Fig. 2 shows the UV-vis absorption spectrum of Chl in 1-butanol. As shown in this figure, Chl absorption exhibits a saddle-like shape with two peaks, respectively, at 415 and 664 nm, from which the absorbed energy can be converted to heat.

To investigate the photothermal effect of Chl, two different laser wavelengths of 661 and 785 nm were used with a power of  $0.1 \text{ kW/m}^2$ . Within each  $150 \mu\text{L}$  sample, 1 mg/mL of Chl solution was dissolved in 1-butanol. 1-butanol was chosen as a solvent since toluene is corrosive to the plastic container. Another reason for using 1-butanol was due to its lower vapor pressure and higher boiling point compared with other solvents of Chl. Figure 3(a) shows the temperature differences of glass samples ( $\Delta T_g$ ) induced by laser irradiation at 661 and 785 nm, respectively. As can be seen in this figure, while a  $\Delta T_g$  of  $9.5 \text{ }^\circ\text{C}$  was generated within 10 min by the 661 nm

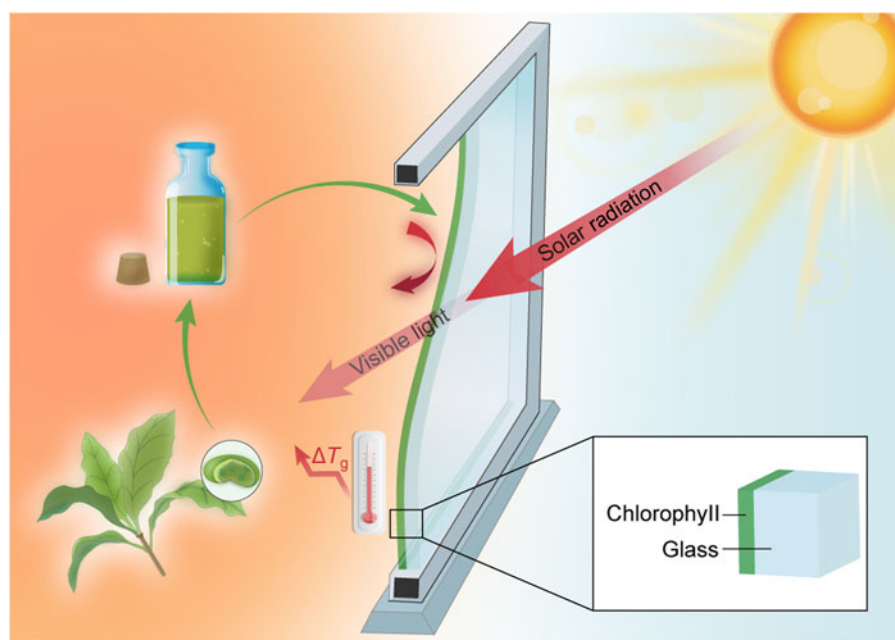
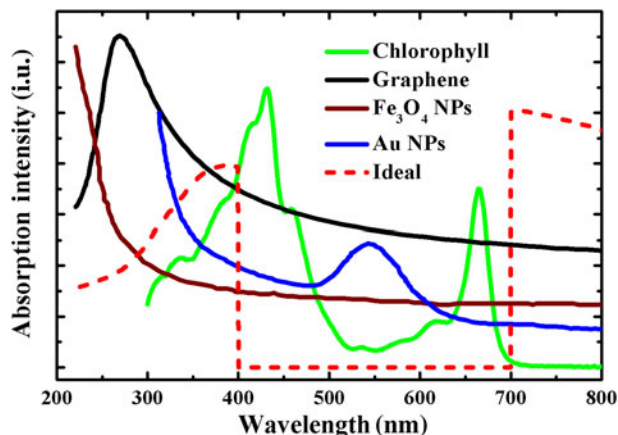


Figure 1. Schematic representation of Chl-coated “Green Window”.



**Figure 2.** Schematic absorption spectra of chlorophyll (solid green), graphene (solid black),  $\text{Fe}_3\text{O}_4$  nanoparticles (solid brown), Au nanoparticles (solid blue), and an ideal absorption curve (dashed red).

laser, much less temperature difference was observed for 785 nm irradiation ( $\sim 1^\circ\text{C}$ ) within the same time period. Quite similar behaviors are observed in Fig. 3(c) for the Chl thin films coated on glass substrates. For a comparative study, the glass samples were sectioned to identical dimensions of  $25\text{ mm} \times 25\text{ mm}$  with a mass density of  $0.15\text{ mg/cm}^2$  Chl. As shown in Fig. 3(b), irradiation with 661 and 785 nm lasers, respectively, give the  $\Delta T_g$  values of 22 and  $2^\circ\text{C}$ . Comparing the results of Figs. 3(a) and 3(b), one can see greater  $\Delta T_g$  generated by the Chl film compared with the solution when using the 661 nm laser. This difference is attributed to the relatively high Chl concentration in the solid film surface. As can also be seen in both Figs. 3(a) and 3(b), the heating curves reach plateaus after 4 min as a result of constant heat loss through the samples.

Multiple layers of Chl thin films on glass substrates were developed to investigate the thickness dependence of the photothermal effect. The multilayer-coating procedures can be found in the Supporting materials. The Chl solution was mixed with PMMA with a ratio of 1:1 and applied uniformly on the glass substrates. Each layer was estimated to have a mass density of  $0.025\text{ mg/cm}^2$  Chl. A Newport 150 W solar simulator was applied with an intensity of  $1\text{ kW/m}^2$  for generating the photothermal effect. Figure 3(c) shows  $\Delta T_g$  versus time for the multilayer samples. Consistently, thicker films (more layers) gave greater  $\Delta T_g$  as expected. Conversely, the thicker films exhibit lower VT. In Figs. 3(a) and 3(c), temperature plateaus can be observed after 2 min of irradiation by laser and solar simulator. This plateau is formed as a result of heat loss through the environment balancing the generation of thermal energy; a rise in temperature no longer observed. Resulting plateaus are shown in Figs. 3(c) and 3(d). Figure 3(d) shows  $\Delta T_{g,\text{max}}$  versus VT for thin films of different layers (a maximum of six layers). Interestingly,  $\Delta T_{g,\text{max}}$  versus VT displays a linear relationship extending to the point where no Chl film is applied (highest VT).

With the  $\Delta T_{g,\text{max}}$  data, U-factor can be calculated for window applications. According to our previous research, only a  $5^\circ\text{C}$  of  $\Delta T_{g,\text{max}}$  can lead to a sufficient decrease in U-factor. Based on the data shown in Figs. 3(c) and 3(d), to generate enough heat for  $5^\circ\text{C}$  of  $\Delta T_{g,\text{max}}$ , a minimum of four layers ( $0.10\text{ mg/cm}^2$ ) of Chl coating is required on the glass for the dimension of  $25\text{ mm} \times 25\text{ mm}$ . According to the data shown in Fig. 3(d),  $5^\circ\text{C}$  of  $\Delta T_{g,\text{max}}$  results in a VT of 70% (the corresponding mass density is  $0.10\text{ mg/cm}^2$  Chl in coating). Compared to most of the double-panes, 70% VT is greatly satisfactory for window applications.<sup>[9]</sup>

Figure 4(a) shows an optical photograph through the Chl film-coated glass with four layers. As can be seen, the image through the “Green Window” is clear and sharp with significant transparency. For comparison, the counterpart image is shown in Fig. 4(b) with a regular glass. The actual “Green Window” sample is shown in Fig. 4(c). As shown in this figure, one can see a quite uniform coating and a smooth surface of the Chl thin film on a glass substrate. Furthermore, no striation can be visually observed. Due to its particular “saddle-like” absorption characteristic, the Chl thin film appears to be green, a natural color of Chl. Figure 4(d) shows the scanning electron microscope (SEM) images of cross-sections of the Chl-coated glass sample (two-layer coating).

### The photothermal properties

The solar photothermal conversion efficiency,  $\eta$ , is defined as the ratio of the energy increase inside the sample to the incident simulated solar radiation. The formula was developed for monochromatic light by Roper et al.,<sup>[16]</sup> and later simplified by Jin et al.<sup>[17]</sup> for solar light:

$$\eta = \frac{(c_g m_g + c_{\text{Chl}} m_{\text{Chl}} + c_{\text{PMMA}}) \Delta T_{g,\text{max}}}{I A \Delta t} \approx \frac{c_g m_g \Delta T_{g,\text{max}}}{I A \Delta t}, \quad (1)$$

where  $c$  ( $\text{J/g}^\circ\text{C}$ ) is the heat capacity and  $m$  (g) is the sample mass. Subscripts (g), (Chl), and (p) correspond to glass, Chl, and PMMA, respectively.  $\Delta T_{g,\text{max}}$  ( $^\circ\text{C}$ ) is the temperature difference between the maximum sample temperature and the ambient temperature;  $\Delta t$  (s) is the time for the sample to reach the maximum temperature;  $I$  ( $\text{W/cm}^2$ ) is the absorbed solar simulator power density, and  $A$  ( $\text{cm}^2$ ) is the irradiated surface area (in this study it is the substrate area). The coating layer volume (containing Chl and PMMA) is negligible in the equation due to its extremely small mass compared with the glass substrate. In this study, the weight of each glass sample,  $m_g$ , is 1.77 g, and the heat capacity of glass,  $c_g$ , is  $0.84\text{ J/g}^\circ\text{C}$ .

Chl’s capacity to absorb solar energy per unit of mass is quantified by specific absorption rate (SAR), which is expressed by the following equation<sup>[17]</sup>:

SAR

$$= \frac{(c_g m_g + c_{\text{Chl}} m_{\text{Chl}} + c_{\text{PMMA}}) \Delta T_{g,\text{max}} - (c_g m_g + c_{\text{PMMA}}) \Delta T_{\text{control}}}{m_{\text{Chl}} \Delta t}, \quad (2)$$

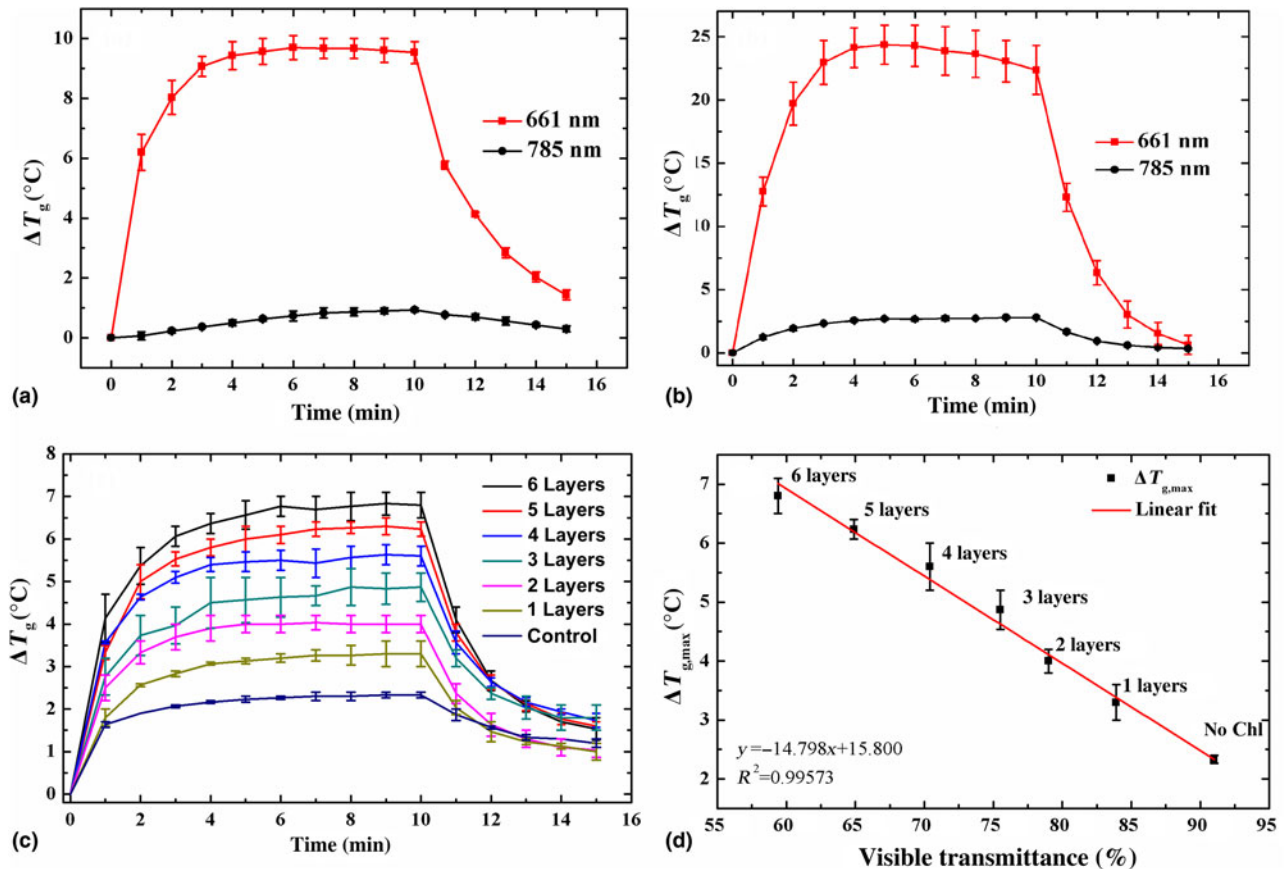


**Figure 3.** (a)  $\Delta T_g$  versus time for Chl in 1-butanol irradiated by 661 and 785 nm lasers. (b)  $\Delta T_g$  versus time for Chl-coated glass irradiated by 661 and 785 nm lasers. (c)  $\Delta T_g$  versus time for Chl-coated glass with different layers of Chl coating irradiated by simulated solar light. (d) Linear  $\Delta T_{g,max}$  versus VT relationship showing the photothermal effects of the glass samples with different thicknesses of Chl coating.

where  $\Delta T_{control}$  is the temperature difference between the maximum temperature that the control (PMMA-coated, without Chl) sample can reach and the ambient temperature. The SAR can be simplified and written as:

$$SAR = \frac{c_g m_g (\Delta T_{g,max} - \Delta T_{control})}{m_{Chl} \Delta t} \quad (3)$$

The rate of window heat loss is given by the standardized thermal transmittance, or U-factor. The U-factor calculation is simplified and generated from ASTM C1199-14<sup>[18]</sup> and the details are included in the Supporting materials. In this study, U-factor is calculated by using the following equation:

$$U = \frac{1}{\frac{1}{1.46 \times ((T_h - T_g)/L)^{0.25} + \sigma e((T_h^4 - T_g^4)/(T_h - T_g))} + \frac{1}{8.07 \times v^{0.605}} + R_L} \quad (4)$$

where  $T_h$  is the indoor air temperature;  $T_g$  is the inner surface

glass temperature;  $H$  is the window height;  $\sigma$  is the Stefan-Boltzmann constant;  $e$  is the emissivity;  $v$  is the wind speed, and  $R_L$  is the resistance of the windowpane assembly.

The solar photothermal conversion efficiency ( $\eta$ ), SAR, and U-factor reduction of each sample with different layers are shown in Table 1. As shown in this table, consistent with the results shown in Figs. 3(a)–3(d),  $\Delta T_{g,max}$  under solar light increases with Chl coating thickness but expectedly with reduced VT. The photothermal conversion efficiency and SAR are seen to be not significantly dependent on the Chl layer thickness. However, the U value is considerably reduced with the increasing Chl mass on the glass substrates, while remaining high VT values for all samples.

According to Carmody et al.,<sup>[19]</sup> the U-factor of an uncoated single-pane window is 4.77 W/m<sup>2</sup>/K. Even for a double-pane window with wood and vinyl frame, the U-factor can be as high as 2.78 W/m<sup>2</sup>/K.<sup>[19]</sup> To achieve Energy Star certification in colder regions of the USA, the Department of Energy requires a window U-factor <1.7 W/m<sup>2</sup>/K (0.3 Btu/h/ft<sup>2</sup>/°F).<sup>[20]</sup> According to our experimental data shown in Table 1, with assumptions of the weather conditions, a single-pane “Green Window” with Chl coatings is characterized by a

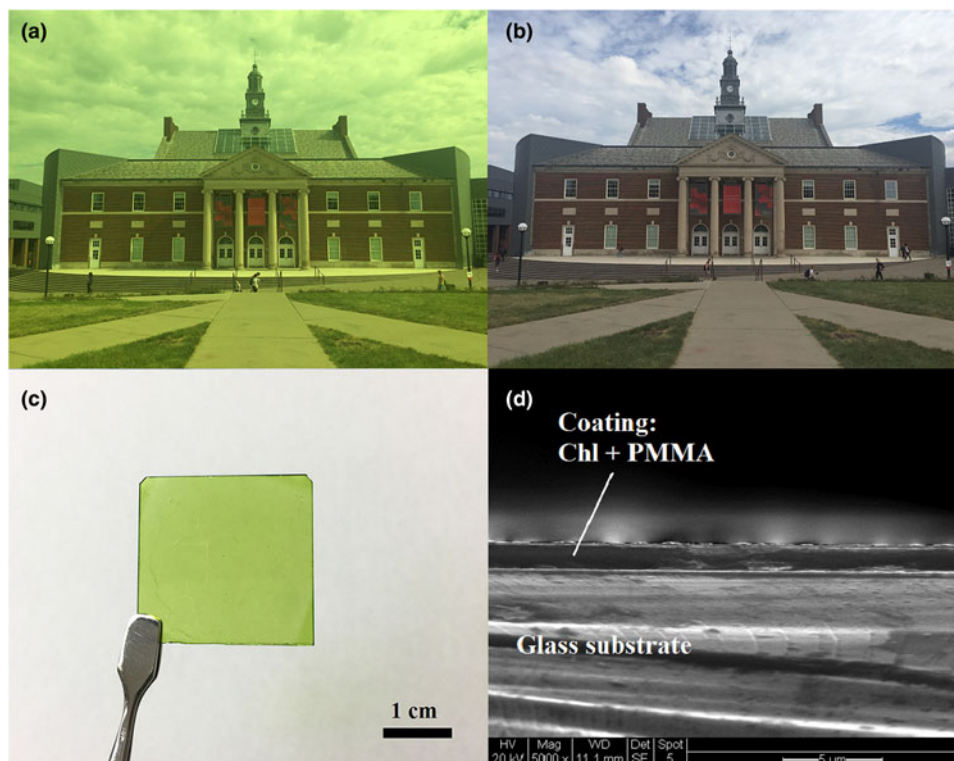


**Figure 4.** Optical photographs showing images through (a) Chl-coated glass with 70% VT; (b) glass without Chl coating, (c) the Chl-coated glass sample with a scale, and (d) SEM image of the cross-section of the two-layer Chl-coated glass.

U-factor as low as  $\sim 1.5 \text{ W/m}^2/\text{K}$  ( $\sim 0.265 \text{ Btu/h/ft}^2/^\circ\text{F}$ ), which is highly satisfactory for the DOE requirements.

### Discussion

As shown in Figs. 3(a) and 3(b), there is a significant difference in  $\Delta T_g$  between irradiations of 661 and 785 nm lasers for both solution and thin film samples. This can be explained by the change in energy conversion efficiency of the two wavelengths as indicated by the absorption spectrum. As can be seen in Fig. 2, Chl typically exhibits two absorption peaks at 415 and 664 nm, respectively. Therefore, by data shown in Figs. 3(a)

and 3(b), stronger photonic absorbance is associated with greater photothermal heating and thus high  $\Delta T_g$  as shown in Figs. 3(a) and 3(b). The laser of 785 nm is, by comparison, weakly absorbed and contributing insignificantly to the photothermal effect. From these experimental observations, one can anticipate an even higher photothermal effect for a laser excitation near the 415 nm peak than observed for the 661 nm laser, since the absorption of Chl at 415 nm is even higher than that at 661 nm, as shown in Fig. 2.

Based on the data shown in Table 1, the Chl-based “Green Window” exhibits an excellent photothermal effect and ideal

**Table 1.** Various parameters of Chl-coated glass samples. (no Chl is the control sample with PMMA coating on glass).

# of layers	$m_{\text{chl}}$ (mg)	$\Delta T_{g,\text{max}}$ ( $^\circ\text{C}$ )	VT (%)	$\eta$ (%)	SAR (W/g)	$U$ ( $\text{W/m}^2/\text{K}$ )
no Chl	0	2.16	90.1	N/A	N/A	1.99
1-layer	0.156	3.13	83.9	15.42	28.55	1.85
2-layer	0.313	4.00	79.0	15.10	28.07	1.75
3-layer	0.469	4.63	75.5	14.99	25.37	1.68
4-layer	0.625	5.47	70.4	14.65	25.69	1.58
5-layer	0.781	6.10	64.9	13.78	24.55	1.50
6-layer	0.938	6.70	59.4	13.09	23.63	1.42

optical properties for window applications, especially for single-pane windows in cold climates. With sufficient self-heating, the U-factor can be significantly lowered, indicating highly improved heat loss in winter. This mechanism lifts the dependence on thermal insulating materials and paves a new path for the novel design of energy-efficient windows. Chl coatings can be applied in a straightforward way onto windows as a retrofit, showing promise in both sustainability and energy efficiency.

Chl coatings are uniquely characterized not only by their strong photon to heat conversion efficiency, but also high VT, an essential quality required for window applications. Compared with other materials that exhibit strong photothermal effects such as gold and Fe<sub>3</sub>O<sub>4</sub> nanoparticles, Chl is much more transparent in the visible band due to its saddle-like absorption spectrum. Moreover, the absorption characteristics of Chl may be modified for further enhanced VT and energy conversion efficiency. Ideally, the width between the two major absorption peaks can be widened, improving VT. The absorptions in the non-visible regions, especially in NIR, can also be enhanced for greater photothermal effect and energy conversion efficiency. Some Chl derivatives such as chlorophyllin and copper Chl have been investigated with quite different absorption spectra.<sup>[21]</sup> Modifications of Chl may result in “red-shift” of the 664 nm absorption peak by substituting magnesium with other NIR absorbers.<sup>[22]</sup> As the green color of Chl originates from strong absorptions in the blue-violet and NIR regions, materials with this optical characteristic may qualify as potential candidates for “Green Window” development, i.e., strongly photothermal while highly transparent. In this fashion, a new approach has been developed in window design, material selection, thermal insulation, and optical tuning.

## Conclusion

As is well known, about 57% of solar light is invisible, but this “free” energy can now be well utilized by the “Green Window” concept via the photothermal effect of natural materials. Inspired by unique optical properties, natural Chl is found to be an ideal coating for energy-efficient window applications. The absorption spectra of naturally occurring Chl optically satisfy the idea of photothermal “Green Window” in both high visible transparency and photon energy conversion. Without relying upon any thermal insulating materials, heat loss can be effectively prevented via reduction of the temperature difference ( $\Delta T$ ) between interior air and window surface. This is achieved by a thin Chl coating that self-heats the window surface while retaining high VT. Experimental results indicate that only a 5 °C temperature increase on the window interior surface is sufficient for a satisfactory U-factor. The profound implication of this study lies with the novel approach in thermal insulation. Without a need for any insulating layers, the U-factor can be significantly reduced, making energy-efficient, single-pane windows highly possible. This novel approach will significantly improve the energy and material savings for regions in

cold climates where thermal transduction plays a substantial role in heat loss.

## Supplementary material

The supplementary material for this article can be found at <https://doi.org/10.1557/mrc.2019.52>

## Acknowledgments

We acknowledge the financial support from the National Science Foundation Grants CMMI-1635089 and EEC-1343568. We thank Dr. Andrew Steckel for the use of the Perkin-Elmer spectrophotometer.

## References

1. ARPA-E: Single-Pan Highly Insulating Efficient Lucid Designs (SHIELD) Program Overview, URL: [https://arpa-e.energy.gov/sites/default/files/documents/files/SHIELD\\_ProgramOverview.pdf](https://arpa-e.energy.gov/sites/default/files/documents/files/SHIELD_ProgramOverview.pdf). [accessed January 20, 2019].
2. J. Han, L. Lu, and H. Yang: Numerical evaluation of the mixed convective heat transfer in a double-pane window integrated with see-through a-Si PV cells with low-e coatings. *Appl. Energy* **87**, 3431–3437 (2010).
3. S.D. Rezaei, S. Shannigrahi, and S. Ramakrishna: A review of conventional, advanced, and smart glazing technologies and materials for improving indoor environment. *Sol. Energy Mater. Sol. Cells* **159**, 26–51 (2017).
4. H. Khandelwal, A.P.H.J. Schenning, and M.G. Debijs: Infrared regulating smart window based on organic materials. *Adv. Energy Mater.* **7**, 1602209 (2017).
5. E. Cuce and P.M. Cuce: Vacuum glazing for highly insulating windows: recent developments and future prospects. *Renewable Sustainable Energy Rev.* **54**, 1345–1357 (2016).
6. A.M. Alkilany, L.B. Thompson, S.P. Boulos, P.N. Sisco, and C.J. Murphy: Gold nanorods: their potential for photothermal therapeutics and drug delivery, tempered by the complexity of their biological interactions. *Adv. Drug Delivery Rev.* **64**, 190–199 (2012).
7. Y. Zhao, M.E. Sadat, A. Dunn, H. Xu, C.-H. Chen, W. Nakasuga, R.C. Ewing, and D. Shi: Photothermal effect on Fe<sub>3</sub>O<sub>4</sub> nanoparticles irradiated by white-light for energy-efficient window applications. *Solar Energy Materials & Solar Cells* **161**, 247–254 (2017).
8. ASTM G173-03(2012), Standard Tables for Reference Solar Spectral Irradiances: Direct Normal and Hemispherical on 37° Tilted Surface. ASTM International (West Conshohocken, PA, 2012).
9. Measuring Performance: Visible Transmittance (VT). EFFICIENT WINDOWS COLLABORATIVE. URL: <http://www.efficientwindows.org/vt.php>. [accessed January 20, 2019].
10. Pilkington: Pilkington K Glass S Brochures. [Online]. Available: <https://www.pilkington.com/en-gb/uk/products/product-categories/thermal-insulation/pilkington-k-glass-range/pilkington-k-glass-s-20->. [Accessed January 20, 2019].
11. X. Huang, P.K. Jain, I.H. El-Sayed, and M.A. El-Sayed: Plasmonic photothermal therapy (PPTT) using gold nanoparticles. *Lasers Med. Sci.* **28**, 217 (2008).
12. X. Huang, I.H. El-Sayed, W. Qian, and M.A. El-Sayed: Cancer cell imaging and photothermal therapy in the near-infrared region by using gold nanorods. *J. Am. Chem. Soc.* **128**, 2115–2120 (2006).
13. M. Chu, Y. Shao, J. Peng, X. Dai, H. Li, Q. Wu, and D. Shi: Near-infrared laser light mediated cancer therapy by photothermal effect of Fe<sub>3</sub>O<sub>4</sub> magnetic nanoparticles. *Biomaterials* **34**, 4078–4088 (2013).
14. K. Yang, S. Zhang, G. Zhang, X. Sun, S.-T. Lee, and Z. Liu: Graphene in mice: ultrahigh in vivo tumor uptake and efficient photothermal therapy. *Nano Lett.* **10**, 3318–3323 (2010).
15. M. Chu, H. Li, Q. Wu, F. Wo, and D. Shi: Pluronic-encapsulated natural chlorophyll nanocomposites for in vivo cancer imaging and photothermal/photodynamic therapies. *Biomaterials* **35**, 8357–8373 (2014).

16. D.K. Roper, W. Ahn, and M. Hoepfner: Microscale heat transfer transduced by surface plasmon resonant gold nanoparticles. *J. Phys. Chem. C* **111**, 3636–3641 (2007).
17. H. Jin, G. Lin, L. Bai, M. Amjad, and E.P.B. Filho: Photothermal conversion efficiency of nanofluids: an experimental and numerical study. *Sol. Energy* **139**, 278–289 (2016).
18. ASTM C1199-14, Standard Test Method for Measuring the Steady-State Thermal Transmittance of Fenestration Systems Using Hot Box Methods. ASTM International (West Conshohocken, PA, 2014).
19. J. Carmody, S. Selkowitz, D. Arasteh, and L. Heschong: *Residential Windows: A Guide to new Technologies and Energy Performance*, 3rd ed. (W. W. Norton & Company, New York, 2007).
20. U. E. P. Agency: Windows, Doors & Skylights Key Product Criteria. URL: [https://www.energystar.gov/products/building\\_products/residential\\_windows\\_doors\\_and\\_skylights/key\\_product\\_criteria](https://www.energystar.gov/products/building_products/residential_windows_doors_and_skylights/key_product_criteria). [accessed September 12, 2018].
21. M. Scotter, L. Castle, and D. Roberts: Method development and HPLC analysis of retail foods and beverages for copper chlorophyll (E141[i]) and chlorophyllin (E141[ii]) food colouring materials. *Food Addit. Contam.* **22**, 1163–1175 (2006).
22. V.P. Perevalov, E.G. Vinokurov, K.V. Zuev, E.A. Vasilenko, and A.Y. Tsivadze: Modification and application of metal phthalocyanines in heterogeneous systems. *Protection of Metals and Physical Chemistry of Surfaces* **53**, 199–214 (2017).